Nonautonomous pulse-driven chaotic oscillator based on Chua's circuit

A. S. Elwakil*

*Department of Electrical and Electronic Engineering, University of Sharjah, P.O. Box 27272, United Arab Emirates (Email: elwakil@ee.ucd.ie , elwakil@sharjah.ac.ae)

Abstract— **A novel nonautonomous chaotic oscillator based on the passive structure of Chua's circuit is proposed. Unlike most of the available members of this class of chaotic oscillators, the proposed circuit is driven by a periodic bipolar pulse-train rather than by sinusoidal excitation. This results in equilibrium points which have fixed positions in space. The circuit employs self feedback via a single comparator, which is the only nonlinear device involved. The output of this comparator is a chaotic bipolar pulse-train. A mathematical model which captures the behavior of the circuit is derived and experimental results are presented. A variant structure with an alternatively excited node is discussed.**

I. INTRODUCTION

Nonautonomous chaotic oscillators form a class of circuits which produce chaos while being driven (excited) by an external time-varying source. While there are many known autonomous chaotic oscillators (see [1] and the references therein), very few nonautonomous chaotic oscillators have been introduced in the literature [2]-[4] following some classical systems, which have been studied in detail [5]-[7]. The reason for such limited number might be the lack of any evidence that the statistical features (eigenvalues, Lyapunov exponents...etc.) of the chaos produced by nonautonomous oscillators possesses any unique property which is not possessed by the chaos produced from autonomous oscillators. Moreover, the performance of nonautonomous oscillators is greatly affected by the quality of the utilized driving force generator.

It can be seen from [2]-[7] that a sinusoidal excitation method has always been adopted in those nonautonomous oscillators which have been reported. This automatically implies that the equilibrium points of these driven systems are time varying. The amplitude and frequency of the sinusoid both contribute to the chaotic dynamics. In [8], the effect of sinusoidal excitation on Chua's circuit was studied. Nonautonomous chaotic oscillators where the driving force is a pulse-train, rather than a sinusoid, have only been proposed in [9] and [10]. In this work, we also aim to present such an oscillator based on the third-order passive structure of Chua's circuit.

Since a bipolar pulse-train switches between two fixed amplitude levels, the corresponding equilibrium points of the circuit remain fixed in space and not time varying. In place of the classical Chua's diode nonlinear resistor [11], we utilize a single comparator as the only nonlinear device in the circuit. Note that a comparator has a nonlinear $V_i - V_o$ characteristic whereas Chua's diode has a nonlinear $V_i - I_i$ characteristic. Therefore, self-feedback is employed from the comparator's output to the excited node.

One main advantage of the proposed chaotic oscillator is its suitability for interfacing with digital circuitry. The driving force can well be a periodic digital clock; the output of the comparator is a chaotic pulse-train compatible with the input levels to a following digital system.

II. PROPOSED NONAUTONOMOUS CHAOTIC OSCILLATOR

Consider the circuit shown in Fig. 1(a) where the passive structure of Chua's circuit, composed of the LC_2 tank resonator, and the RC_1 low-pass filter section, can be clearly recognized. The output of a comparator, which is controlled via the voltage across C_1, is fedback to the excited node via resistor R_F. The driving force V_P is a pulse-train coupled via R_S to the same node. The output levels of both V_P and the comparator are bipolar and equal $\pm V_{CC}$, where $\pm V_{CC}$ are the bias supplies for the comparator chip. The circuit in Fig. 1 is therefore described by:

$$L\dot{I}_L = V_{C2} \tag{1}$$

0-7803-7761-3/03/$17.00 ©2003 IEEE

$$C_2\dot{V}_{C2} = \frac{V_{C1}}{R} - (\frac{1}{R} + \frac{1}{R_S} + \frac{1}{R_F})V_{C2} - I_L + \frac{V_P}{R_S} + \frac{V_N}{R_F} \quad (2)$$

$$C_1\dot{V}_{C1} = \frac{V_{C2} - V_{C1}}{R} \quad (3)$$

where V_N and V_P are the output voltages of the comparator and the driving pulse-train, expressed respectively as:

$$V_N = V_{CC} \cdot \mathrm{sgn}(V_{C1}) = \begin{cases} V_{CC} & V_{C1} \geq 0 \\ -V_{CC} & V_{C1} < 0 \end{cases} \quad (4)$$

$$V_P = V_{CC} \cdot \mathrm{sgn}(\sin(\omega_P t)) \quad (5)$$

Here, ω_P is the frequency of oscillation of the pulse-train.

By introducing the following dimensionless variable: $x = \frac{V_{C1}}{V_{CC}}$, $y = \frac{V_{C2}}{V_{CC}}$, $z = \frac{RI_L}{V_{CC}}$, $\tau = \omega_P t$, $\epsilon_c = \frac{C_1}{C_2}$, $\alpha_1 = \frac{L\omega_P}{R}$, $\alpha_2 = RC_2\omega_P$, $\beta_F = \frac{R}{R_F}$ and $\beta_S = \frac{R}{R_S}$, the above set of equations transform into:

$$\begin{pmatrix} \dot{x} \\ \dot{y} \\ \dot{z} \end{pmatrix} = \begin{pmatrix} \frac{-1}{\epsilon_c\alpha_2} & \frac{1}{\epsilon_c\alpha_2} & 0 \\ \frac{1}{\alpha_2} & \frac{1+\beta_F+\beta_S}{-\alpha_2} & \frac{-1}{\alpha_2} \\ 0 & \frac{1}{\alpha_1} & 0 \end{pmatrix} \begin{pmatrix} x \\ y \\ z \end{pmatrix} + \begin{pmatrix} 0 \\ \frac{a}{\alpha_2} \\ 0 \end{pmatrix} \quad (6)$$

Note that all the parameters (α_1, α_2, β_F, β_S) in the above state transition matrix are constants which are independent of the state of the comparator output or the driving force. The only parameter in (6) which depends on these two outputs is a, which is a switching constant given by:

$$a = \begin{cases} \beta_F + \beta_S P(\tau) & X \geq 0 \\ -\beta_F + \beta_S P(\tau) & X < 0 \end{cases} \quad (7a)$$

$$\text{and } P(\tau) = \mathrm{sgn}(\sin\tau) = \begin{cases} 1 & \sin\tau \geq 0 \\ -1 & \sin\tau < 0 \end{cases} \quad (7b)$$

Since a does not appear in the state transition matrix, it has no effect on the dynamics of the system at the equilibrium points. It is clear that this switching constant will only affect the position in space of the equilibrium points of the system, which are given by: $(x_0, y_0, z_0) = (0, 0, a)$. Using (7), it is seen that there are in general four equilibrium points; two located in the positive x half-space equal to $(0, 0, \beta_F \pm \beta_S)$ and two located in the negative x half-space equal to $(0, 0, -\beta_F \pm \beta_S)$. In the special case where $\beta_F = \beta_S = \beta$, two of these points coincide with the origin. Effectively, the system has three equilibrium points in this case; the origin and $(0, 0, \pm 2\beta)$.

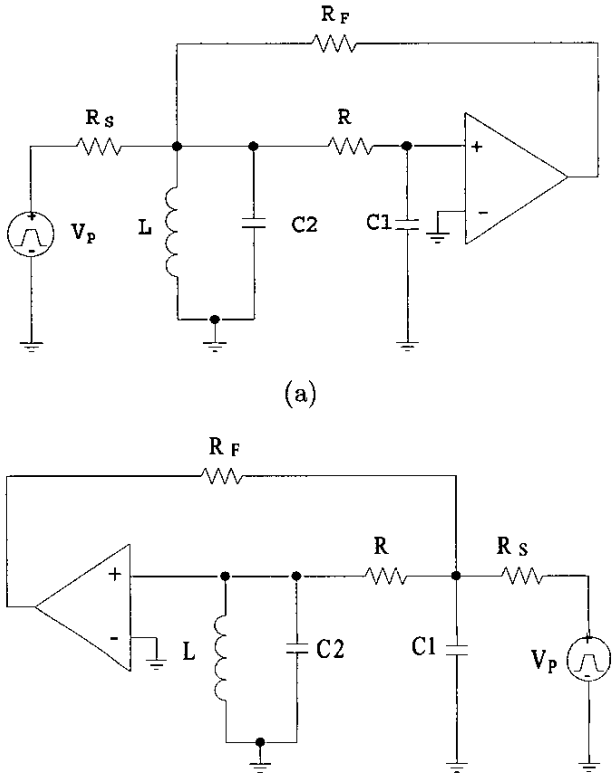

Figure1: Proposed pulse-driven nonautonomous chaotic oscillator: (a) circuit structure with excitation across C_2; (b) alternative structure with excitation across C_1.

Numerical simulations of the above model were performed using a Runge-Kutta algorithm with 0.001 step size and taking $\alpha_1 = 0.05$, $\alpha_2 = 50$, $\beta_F = \beta_S = 3$, $\tau = 0.1t$ and $\epsilon_c = 0.2$. In Fig. 2(a), the observed $y - z$ projection of the chaotic attractor is shown. Note that the three equilibrium points in this case are the origin and $(0, 0, \pm 6)$, which are clearly visible in the plot. In Figs. 2(b) and (c), the same projection is shown for the two cases: $(\beta_F, \beta_S) = (2, 3)$ and $(3, 2)$ respectively. The equilibrium points in both cases are $(0, 0, \pm 1)$ and $(0, 0, \pm 5)$. Note that the condition $\beta_F > \beta_S$ implies

that the two equilibrium points in the region $x > 0$ ($x < 0$) also lie in the region $z > 0$ ($z < 0$) while the condition $\beta_F < \beta_S$ implies alternating equilibrium points, i.e. when x switches from the positive to the negative half-space, z will switch in the opposite direction.

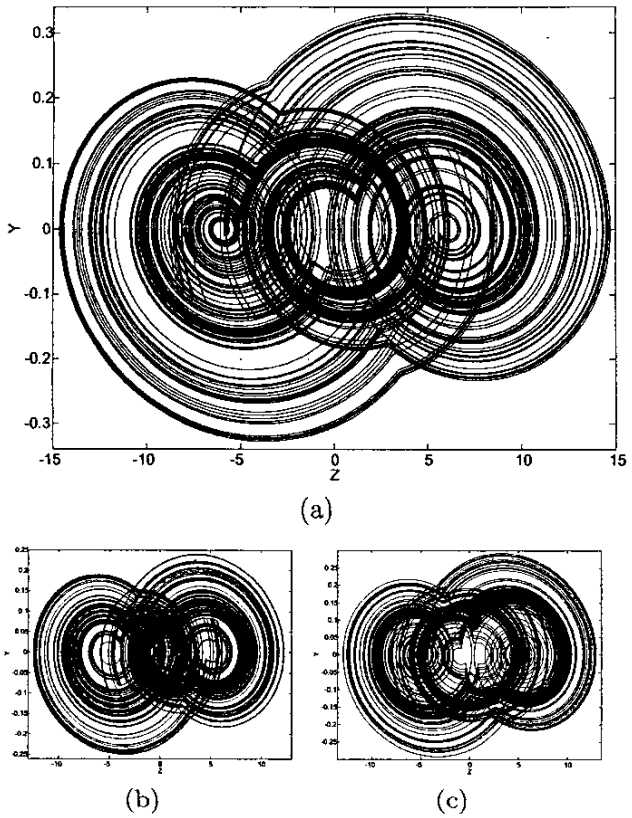

Figure2: $y - z$ projection of the chaotic attractor obtained via numerical integration of (6) ($\alpha_1 = 0.05$, $\alpha_2 = 50$, $\epsilon_c = 0.2$): (a) $(\beta_F, \beta_S) = (3,3)$; (b) $(\beta_F, \beta_S) = (2,3)$ and (c) $(\beta_F, \beta_S) = (3,2)$.

An experimental setup of Fig. 1(a) was constructed taking $L = 1mH$, $C_1 = 10nF$, $C_2 = 100nF$, $R = 5k\Omega$ and using a general purpose TL082 op amp as the comparator. We have chosen to fix R_F at $1k\Omega$ and use a variable $5k\Omega$ resistor for R_S in order to tune the circuit dynamics. Noting that the resonant frequency of the LC_2 tank is approximately $16kHz$, the frequency of the driving pulse generator was scanned over the range $1kHz - 20kHz$. The comparator was biased from $\pm 5V$ supplies and the pulse generator output was also fixed to $\pm 5V$.

We have observed chaos in the range of frequencies $4kHz - 18kHz$. In Fig. 3(a), the period-one orbit observed at $5kHz$ with $R_S = 1.528k\Omega$ is shown. The period-two orbit in Fig. 3(b) is born at $R_S = 1.568k\Omega$ whereas the chaotic trajectory in Fig. 3(c) corresponds to $R_S = 1.636k\Omega$. All projections represent the $V_{C1} - V_{C2}$ $(x - y)$ phase plane since it is particularly difficult to measure the current in the inductor I_L (z). In Fig. 3(d), a sample of the chaotic pulse-train generated at the comparator's output is shown. When the frequency of the pulse generator is increased to $15kHz$ with $R_S = 1.907k\Omega$ and $R = 7.6k\Omega$, we observe the double-scroll-like attractor shown in Fig. 4(a). The single-scroll, shown in Fig. 4(b), appears when R_S is increased to $1.952k\Omega$. It is worth noting that the chaotic pulse-train generated at the comparator's output can be used in place of classical digital pseudo-random generators to feed a following digital circuit.

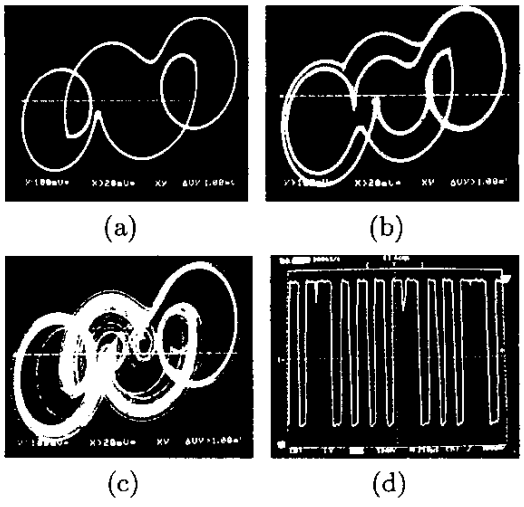

Figure 3: Experimental $V_{C1} - V_{C2}$ observations $(Xaxis : 20mV/div, Yaxis : 100mV/div)$ (a) period-1 orbit (b) period-2 orbit (c) chaotic trajectory (d) sample chaotic pulse output waveform of the comparator $(Xaxis : 250\mu s/div, Yaxis : 1V/div)$.

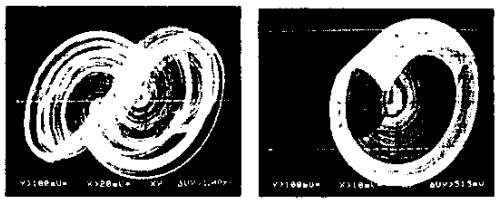

Figure 4: Experimental observations at $15kHz$ driving force frequency $(Xaxis : 20mV/div, Yaxis : 100mV/div)$. (a) double-scroll-like attractor and (b) single-scroll attractor.

III. Alternative configuration

The passive structure of Chua's circuit is a two-node structure. In Fig. 1(a), we have chosen to excite one of these nodes, namely the one across C_2. Here, we demonstrate the possibility of exciting the alternative node, i.e. the one across C_1. The circuit structure in this case is shown in Fig. 1(b) and is described by:

$$\begin{pmatrix} \dot{x} \\ \dot{y} \\ \dot{z} \end{pmatrix} = \begin{pmatrix} \frac{1}{\epsilon_c} & \frac{-(1+\beta_F+\beta_S)}{\epsilon_c} & 0 \\ \frac{1}{\alpha_2} & \frac{-1}{\alpha_2} & \frac{-1}{\alpha_2} \\ 0 & \frac{1}{\alpha_1} & 0 \end{pmatrix} \begin{pmatrix} x \\ y \\ z \end{pmatrix} + \begin{pmatrix} a \\ 0 \\ 0 \end{pmatrix} \quad (8)$$

where a is as given by (7) with the switching condition dependent on y instead of x.

Numerical integration of the above equation was carried out after setting $\epsilon_c = 0.1$, $\alpha_1 = 0.07$, $\alpha_2 = 0.5$ and $\beta_F = \beta_S = 3$. For clarity, the observed projection of the chaotic attractor in the $x - y - z$ subspace is shown in Fig. 5. The four equilibrium points of the system in this subspace are given by: $(x_0, y_0, z_0) = (-a, 0, -a)$ which are also fixed in space but are different from the ones offered by the previous node excitation. A single positive Lyapunov exponent equal to 0.0089 was also calculated from the y time series.

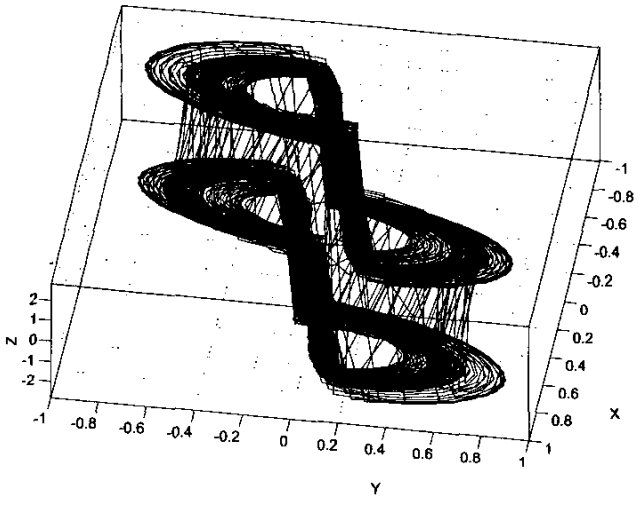

Figure 5: $x - y - z$ subspace chaotic attractor observed from the model of the alternatively excited circuit in Fig. 1(c).

IV. Conclusion

A pulse-driven nonautonomous chaotic oscillator with equilibrium points fixed in space was proposed. A basic advantage of this oscillator is its suitability for interconnection with digital circuits. It is clear that the number of equilibrium points in space are directly proportional to the sum of the possible voltage output levels of both the comparator and the driving pulse-train. Hence, if multi-level-logic is adopted, the number of equilibrium points can be increased.

References

[1] A. S. Elwakil and M. P. Kennedy, Construction of classes of circuit-independent chaotic oscillators using passive-only nonlinear devices, *IEEE Trans. Circuits & Syst.-I* 48 (2001) 289-307.

[2] A. Azzouz, R. Duhr and M. Hasler, Transition to chaos in a simple nonlinear circuit driven by a sinusoidal voltage source, *IEEE Trans. Circuits & Syst.-I* 30 (1983) 913-914.

[3] K. Murali, M. Lakshmanan and L. O. Chua, The simplest dissipative nonautonomous chaotic circuit, *IEEE Trans. Circuits & Syst.-I* 41 (1994) 462-463.

[4] J. G. Lacy, A simple piece-wise-linear nonautonomous circuit with chaotic behavior, *Int. J. Bifurcation & Chaos* 6 (1996) 2097-2100.

[5] M. P. Kennedy and L. O. Chua, Van der Pol and chaos, *IEEE Trans. Circuits & Syst.-I* 33 (1983) 974-980.

[6] S. Tanaka, T. Matsumoto and J. Noguchi, Multi-folding: alternative appearing of period-one attractors and chaotic attractors in a driven R-L-diode circuit, *Physics Letters A* 157 (1991) 37-42.

[7] S. Tanaka, J. Noguchi, S. Higuchi and T. Matsumoto, A repeated appearance of period-1 attractor in a driven R-L-diode circuit: experimental and theoretical bifurcation analysis, *IEICE Trans. Fundamentals* E74 (1991) 1406-1413.

[8] K. Murali and M. Lakshmanan, Effect of sinusoidal excitation on Chua's circuit, *IEEE Trans. Circuits & Syst.-I* 39 (1992) 264-270.

[9] T.Saito and M.Oikawa, Chaos and fractals from a forced artificial neural cell, *IEEE Trans. Neural Networks* 4 (1993).42-52.

[10] K. Miyachi, H.Nakano and T.Saito, Response characteristics of a chaotic spiking oscillator, Proc. of IJCNN, Honolulu, (2002) 2726-2731.

[11] M. P. Kennedy, Robust op amp realization of Chua's circuit, *Frequenz* 46 (1992) 66-80.

[12] M. P. Kennedy and L. O. Chua, Hysteresis in electronic circuits: a circuit theorist's perspective, *Int. J. Circuit Theory & Applications* 19 (1991) 471-515.

[13] A. S. Elwakil, Low-voltage relaxation oscillator, *Electronics Letters* 36 (2000) 1256-1257.

[14] A. S. Elwakil and M. P. Kennedy, Improved implementation of Chua's chaotic oscillator using the current feedback op amp, *IEEE Trans. Circuits & Syst.-I* 47 (2000) 76-79.

[15] A. S. Elwakil and M. P. Kennedy, Inductorless hyperchaos generator, *Microelectronics Journal* 30 (1999) 739-743.